


 Cite this: *RSC Adv.*, 2025, 15, 5837

# Sensitive determination of valganciclovir via Ni–Co multilayer nanowire-modified carbon paste electrode

 Maedeh Malekzadeh,<sup>a</sup> Amir Abbas Rafati \*<sup>a</sup> and Ahmad Bagheri <sup>b</sup>

This study presents the development of an electrochemical sensor based on a carbon paste electrode modified with nickel–cobalt multilayer nanowires (Co–Ni(MLNW)/CPE) for the detection of valganciclovir, an antiviral drug. The sensor was fabricated using an electrochemical deposition method, and its electrochemical behavior was investigated through cyclic voltammetry (CV) and differential pulse voltammetry (DPV). The influence of pH on the sensor's performance was extensively studied, revealing that the redox reaction of valganciclovir (VGCV) involves proton exchange, making pH optimization crucial. The results demonstrated that the sensor exhibited a wide linear range from 0.1 to 2000 nM, with a low detection limit of 0.03 nM at pH 7, the optimal condition for VGCV detection. Additionally, the sensor showed excellent stability, reproducibility, and selectivity, with negligible interference from common ions and biological molecules. The sensor's applicability was further validated through the determination of VGCV in human plasma samples, achieving a high recovery rate of 97.9%. These findings indicate that the proposed Co–Ni(MLNW)/CPE sensor is a promising tool for the accurate, sensitive, and reliable determination of VGCV in clinical and pharmaceutical settings.

 Received 17th November 2024  
 Accepted 14th February 2025

DOI: 10.1039/d4ra08155b

[rsc.li/rsc-advances](https://rsc.li/rsc-advances)

## 1. Introduction

Valganciclovir (VGCV) (Scheme 1) is a crucial antiviral medication, particularly for treating and preventing cytomegalovirus (CMV) infections in immunocompromised individuals, such as AIDS patients and organ transplant recipients.<sup>1</sup> Precise monitoring of VGCV levels is essential for effective therapeutic management. Suboptimal dosing can lead to viral resistance, while excessive levels can cause toxic side effects.<sup>2</sup> Consequently, developing reliable and sensitive analytical methods for determining VGCV concentrations in biological samples is of paramount importance.<sup>3</sup>

Conventional VGCV quantification methods, like high-performance liquid chromatography (HPLC), although accurate, often involve time-consuming procedures, high costs, and require sophisticated instrumentation.<sup>4–6</sup> Electrochemical sensing offers a promising alternative due to its inherent advantages, including simplicity, cost-effectiveness, rapid response, and suitability for on-site analysis.<sup>7–11</sup> Modifying electrodes has further enhanced the sensitivity and selectivity of electrochemical sensors, enabling the detection of trace levels of pharmaceutical compounds in complex matrices, such as human plasma.<sup>12–16</sup> The application of nanomaterials in sensor

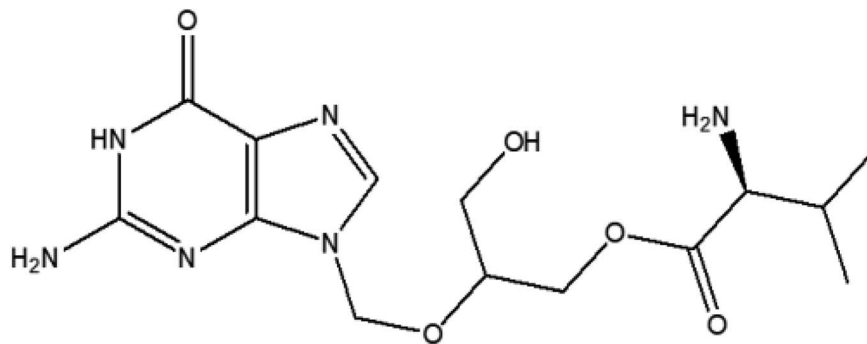
design has attracted considerable attention due to their unique properties, including high surface area, enhanced conductivity, and facilitation of electron transfer processes.<sup>17–20</sup> Among these, metallic nanowires have demonstrated significant potential for improving electrochemical sensor performance. Nickel–cobalt multilayer nanowires (Co–Ni(MLNW)), in particular, are recognized for their exceptional electrochemical properties, including high catalytic activity and excellent stability.<sup>21–23</sup> Incorporating these nanowires into carbon paste electrodes (CPEs) can significantly enhance the electrode's sensitivity, making them ideal for detecting low concentrations of antiviral drugs like VGCV.<sup>24–26</sup>

This study reports the development of a novel electrochemical sensor based on a carbon paste electrode modified with Ni–Co multilayer nanowires (Co–Ni(MLNW)/CPE) for the sensitive and selective determination of VGCV. The sensor's performance was evaluated using differential pulse voltammetry (DPV), a technique known for its high sensitivity and low detection limits.<sup>27</sup> We have characterized the morphology of the Ni–Co MLNWs and the modified electrode surface using scanning electron microscopy (SEM) and energy-dispersive X-ray spectroscopy (EDX) techniques. The proposed sensor demonstrated excellent analytical characteristics, including a wide linear dynamic range, a low detection limit, and good reproducibility. The sensor's applicability was validated by successfully detecting VGCV in human plasma samples, achieving a high recovery rate, thus highlighting its potential for routine clinical analysis. This research aims to provide a sensitive,

<sup>a</sup>Department of Physical Chemistry Faculty of Chemistry and Petroleum Sciences, Bu-Ali Sina University, P. O. Box 65174, Hamedan, Iran. E-mail: [aa\\_rafati@basu.ac.ir](mailto:aa_rafati@basu.ac.ir); Fax: +98-81-3140 8025

<sup>b</sup>Department of Chemistry, Semnan University, Semnan, Iran





Scheme 1 Structure of valganciclovir (VGCV).

selective, and cost-effective method for VGCV determination, which could be used in clinical settings to monitor drug levels in patients, ensuring optimal therapeutic outcomes. This study presents, for the first time, the application of a Ni–Co multilayer nanowire-modified carbon paste electrode (Ni–Co MLNW/CPE) for the sensitive and selective electrochemical determination of valganciclovir. The unique combination of the high catalytic activity and stability of Ni–Co multilayer nanowires with the simplicity and cost-effectiveness of a carbon paste electrode offers a promising new approach for VGCV detection.

## 2. Experimental section

### 2.1. Reagents and materials

All chemicals used were of analytical grade and used as received without further purification. These included cobalt(II) sulfate heptahydrate ( $\text{CoSO}_4 \cdot 7\text{H}_2\text{O}$ ), nickel(II) sulfate hexahydrate ( $\text{NiSO}_4 \cdot 6\text{H}_2\text{O}$ ), boric acid ( $\text{H}_3\text{BO}_3$ ), and phosphoric acid ( $\text{H}_3\text{PO}_4$ ) (all from Sigma-Aldrich). Deionized water (Millipore, resistivity  $>18 \text{ M}\Omega \text{ cm}^{-1}$ ) was used throughout. A 50 mM phosphate buffer solution (PBS) at pH 7.0 was prepared by dissolving appropriate amounts of sodium phosphate monobasic and sodium phosphate dibasic in deionized water. The pH was adjusted using diluted phosphoric acid or sodium hydroxide solutions as needed. High-purity nitrogen gas (99.99%) was used for deoxygenating solutions. Human plasma was obtained from Central Hamedan Clinical and Pathological Laboratory (Hamedan, Iran) and stored in refrigerator immediately after collection before used.

### 2.2. Instrumentation

Electrochemical measurements were performed using a Micro-Autolab potentiostat–galvanostat (Metrohm, The Netherlands) controlled by NOVA 1.7 software. A conventional three-electrode system was employed: a modified carbon paste electrode (CPE) as the working electrode, a platinum wire as the counter electrode, and a silver/silver chloride electrode ( $\text{Ag}/\text{AgCl}$ , 3 M KCl) as the reference electrode. All measurements were performed at room temperature. The peak currents obtained from the voltammograms were used to construct calibration curves for the quantification of VGCV. The detection limit was calculated based on the signal-to-noise ratio ( $S/N = 3$ ).

### 2.3. Synthesis of nickel–cobalt multilayer nanowires

Nickel–cobalt multilayer nanowires (Ni–Co MLNWs) were synthesized *via* electrodeposition using commercially available anodized aluminum oxide (AAO) membranes (Whatman, Anodisc 13 with pore diameter: 0.1  $\mu\text{m}$ , pore length: 60  $\mu\text{m}$ ) as templates. Prior to electrodeposition, a thin layer of gold was sputtered onto one side of the AAO membrane to provide an electrically conductive substrate. Electrodeposition was carried out in a two-electrode configuration with the AAO template (gold-sputtered side) as the working electrode and a platinum plate as the counter electrode. The electrolyte solutions consisted of 0.1 M  $\text{NiSO}_4 \cdot 6\text{H}_2\text{O}$  and 0.1 M  $\text{CoSO}_4 \cdot 7\text{H}_2\text{O}$ . Nickel and cobalt layers were deposited alternately by immersing the AAO template in the respective solutions. A constant potential of  $-2.5 \text{ V}$  (optimized based on previously published articles)<sup>28</sup> was applied for 60 seconds for each metal deposition, with a total of 15 cycles, resulting in a 30 minutes deposition process. Following electrodeposition, the AAO template was selectively dissolved in a 3 M NaOH solution at 60  $^\circ\text{C}$  for 24 hours to release the Ni–Co MLNWs. The resulting nanowires were then washed several times with deionized water and ethanol and dried under vacuum at room temperature.

### 2.4. Fabrication of the modified carbon paste electrode

The modified carbon paste electrode (Ni–Co MLNW/CPE) was prepared by thoroughly mixing graphite powder (Sinchem, Korea), paraffin oil (Sigma-Aldrich), and the synthesized Ni–Co MLNWs in a weight ratio of 60:25:15. The mixture was homogenized manually for 15 minutes to ensure a uniform distribution of the nanowires within the carbon paste matrix. The resulting paste was then packed tightly into the cavity of a 1 mL syringe (cut tip), with a copper wire inserted through the back to establish electrical contact. The electrode surface was polished on a smooth paper surface until a shiny appearance was achieved.

### 2.5. Electrochemical measurements

Electrochemical measurements were performed using cyclic voltammetry (CV) and differential pulse voltammetry (DPV). The potential scan rate for CV was 50  $\text{mV s}^{-1}$  unless otherwise stated. For DPV, the following optimized parameters were used:



potential was registered from 0.4 to 1.4 V at a sweep rate of  $50 \text{ mV s}^{-1}$ ; the pulse height and width were set as 50 mV and 50 ms, respectively. Prior to each electrochemical measurement, the electrolyte solution was deoxygenated by purging with nitrogen gas for 10 minutes. The performance of the Ni-Co MLNW/CPE was evaluated by analyzing various concentrations of VGCV in the prepared PBS.

## 2.6. Characterization of Ni-Co MLNWs and modified electrode

The morphology and structure of the synthesized Ni-Co MLNWs were characterized by SEM and EDX analyses (VEGA TESCAN SEM, Czech Republic).

## 2.7. Analysis of VGCV in human plasma

To assess the practical applicability of the developed sensor, VGCV was determined in human plasma samples. A protein precipitation procedure was employed to remove interfering proteins. Briefly,  $20 \mu\text{L}$  of 20% (v/v) perchloric acid was added to 1 mL of plasma. The mixture was vortexed for 30 seconds and centrifuged at 6000 rpm for 5 minutes. The supernatant was then carefully collected and diluted with PBS (pH 7.0) to an appropriate concentration range for analysis. VGCV concentrations were determined using the standard addition method. The accuracy of the method was evaluated by calculating the recovery of spiked VGCV in the plasma samples.

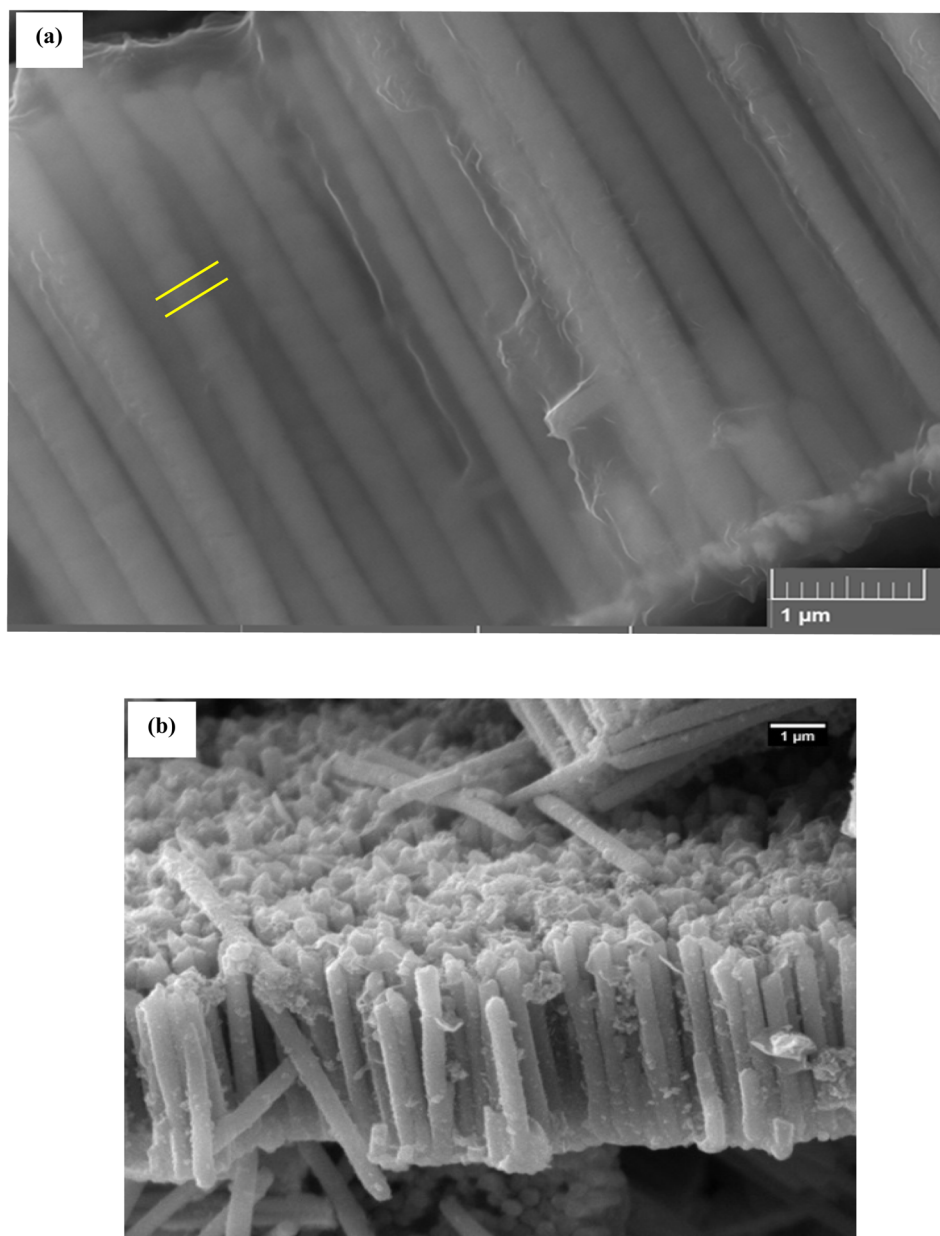


Fig. 1 SEM images of (a) Co-Ni multilayer nanowires; (b) Co-Ni alloy nanowires prepared in the AAO template and released from template by dissolving the template in NaOH.



### 3. Results and discussion

#### 3.1. Characterization of fabricated nanowires

In this study, a detailed characterization of nickel–cobalt nanowires with both multilayered and alloyed structures was conducted to compare their structural and compositional properties. The nanowires were synthesized *via* electrodeposition using AAO templates as described in the Methods section. Two modified carbon paste electrodes (CPEs) were prepared separately using these nanowires to explore the impact of their different structures on electrochemical performance.

The morphological characteristics of the multilayered and alloyed nickel–cobalt nanowires were examined using Scanning Electron Microscopy (SEM). The SEM images were obtained with partially dissolved AAO templates to provide a clearer view of the nanowires. However, the templates were fully dissolved prior to their use in the modified electrodes to prevent any interference with the electrochemical performance. The SEM

images, shown in Fig. 1, reveal that the average diameter of both types of nanowires was approximately 300 nm. Fig. 1(a) displays the SEM image of the multilayered nickel–cobalt nanowires. These nanowires were synthesized by alternating layers of nickel and cobalt, with 15 cycles of deposition, each layer being deposited for 1 minute. The clear distinction between the layers is evident, indicating successful formation of the multilayer structure.

Fig. 1(b) shows the SEM image of the alloyed nickel–cobalt nanowires, which were synthesized from a mixed electrolyte solution containing both nickel(II) sulfate and cobalt(II) sulfate. The alloyed structure lacks the distinct layer separation seen in the multilayered nanowires, consistent with the expected morphology of an alloy.

EDX was employed to determine the elemental composition of the synthesized nanowires. The EDX spectra for both types of nanowires are presented in Fig. 2. Fig. 2(a) shows the EDX spectrum for the multilayered nickel–cobalt nanowires. The

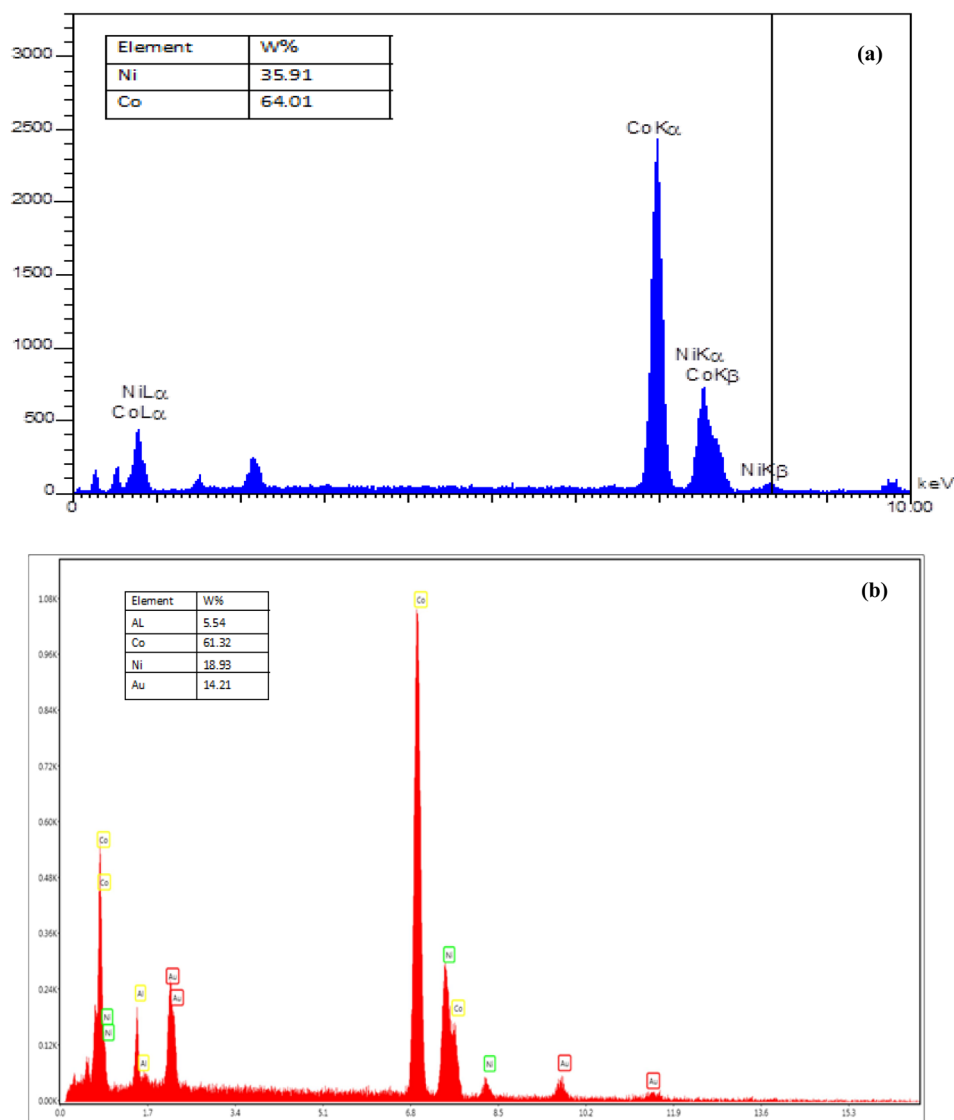


Fig. 2 EDX analysis results of: (a) Co–Ni multilayer nanowires; (b) Co–Ni alloy nanowires.



analysis reveals that these nanowires consist of 35.91 wt% nickel and 64.01 wt% cobalt. The presence of aluminum peaks is attributed to incomplete dissolution of the AAO template, while the gold peak results from the gold sputtering process used during sample preparation. Fig. 2(b) displays the EDX spectrum for the alloyed nickel–cobalt nanowires. These nanowires have a composition of 18.93 wt% nickel and 61.32 wt% cobalt. The higher cobalt content relative to nickel in the alloyed nanowires is likely due to the faster electrodeposition rate of cobalt compared to nickel, which leads to a predominance of cobalt in the final composition.

The compositional differences between the multilayered and alloyed nanowires are significant, highlighting the influence of

the electrodeposition process on the resulting nanostructures. The distinct layering in the multilayered nanowires contrasts with the more homogeneous alloyed structure, which may impact their electrochemical behavior and suitability for specific applications.

### 3.2. Electrochemical behavior of the modified electrode

**3.2.1. Response of the designed electrode to VGCV.** The electrochemical response of the modified electrode to the antiviral drug VGCV was investigated using cyclic voltammetry (CV) and differential pulse voltammetry (DPV). The oxidation peak of VGCV was observed within the potential range of 0.8 to 1.3 V, and

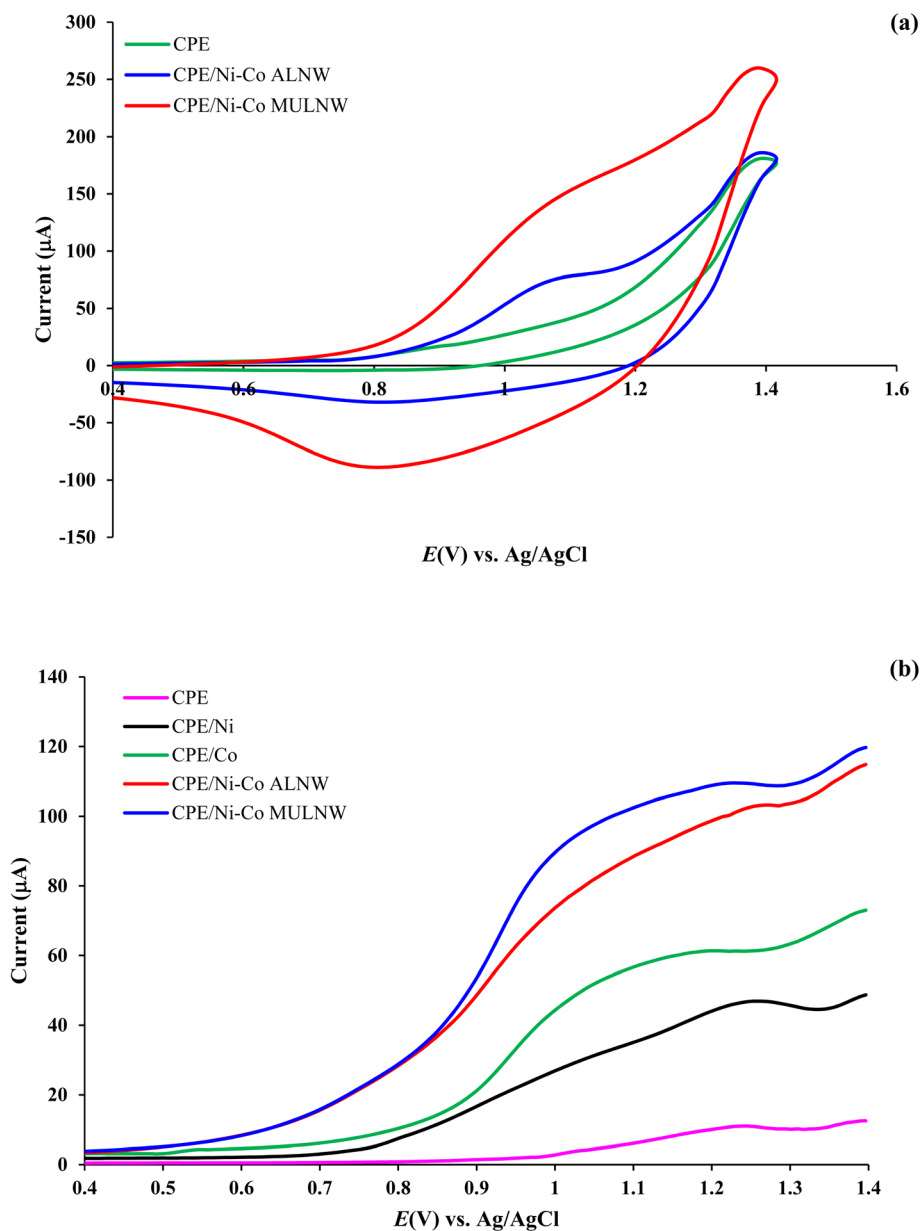


Fig. 3 (a) Cyclic voltammograms of VGCV recorded at the surface of different fabricated electrodes; (b) comparison DPV response of CPE, CPE/Ni, CPE/Co, Co–Ni(ALNW)/CPE and Co–Ni(MLNW)/CPE electrodes. The concentration of VGCV is 900 nM in PBS 0.1 M (pH 7.4) at a scan rate of  $100 \text{ mV s}^{-1}$ .



the reduction peak appeared between 0.6 to 1.2 V. Fig. 3(a) shows the CV responses of three electrodes: unmodified CPE, CPE modified with multilayered nickel-cobalt nanowires (Co-Ni(MLNW)/CPE), and CPE modified with alloyed nickel-cobalt nanowires (Co-Ni(ALNW)/CPE) in the presence of 850 nM VGCV in phosphate buffer solution (pH 7.4) at a scan rate of 100 mV s<sup>-1</sup>. The unmodified CPE showed a weak response with only an oxidation peak. In contrast, the modified electrodes, particularly Co-Ni(MLNW)/CPE, displayed both oxidation and reduction peaks with significantly enhanced current, indicating improved electrocatalytic activity towards VGCV.

Fig. 3(b) present the DPV responses for the oxidation of VGCV. The absence of peaks in the phosphate buffer alone confirmed that the observed peaks were solely due to the presence of VGCV. The shift of the oxidation potential to lower values for the modified electrodes suggests that the nickel-cobalt nanowires enhance the electrocatalytic oxidation of VGCV. Among the tested electrodes, Co-Ni(MLNW)/CPE was selected for further experiments due to its superior performance.

To optimize the modified electrode for VGCV detection, the impact of each modification step was analyzed. Five different electrodes were prepared: unmodified CPE, CPE modified with nickel (CPE/Ni), CPE modified with cobalt (CPE/Co), CPE modified with multilayered nickel-cobalt nanowires (Co-Ni(MLNW)/CPE), and CPE modified with alloyed nickel-cobalt nanowires (Co-Ni(ALNW)/CPE). Both nickel and cobalt individually improved the electrochemical response, with cobalt showing a more pronounced effect. The combination of nickel and cobalt nanowires further enhanced the electrode's performance, demonstrating a synergistic effect between the two nanostructures.

The increased surface area and excellent electrical conductivity of the nanowires contributed to the enhanced current observed for the CPE/Ni-Co modified electrodes compared to the unmodified CPE and those modified with either nickel or cobalt alone. The best response to VGCV was achieved with the Co-Ni(MLNW)/CPE, indicating its high electrocatalytic capability for the electrochemical oxidation of VGCV. These findings suggest that the optimized Co-Ni(MLNW)/CPE electrode is highly suitable for the direct determination of VGCV concentrations.

**3.2.2. Effect of pH on the performance of Co-Ni(MLNW)/CPE sensor for VGCV detection.** The pH of the analyte solution is a crucial parameter in electrochemical studies, particularly regarding the redox behavior of electroactive species. The acidity or alkalinity of the solution significantly influences the peak potentials of oxidation and reduction reactions, especially for species that undergo proton exchange during the redox process. For VGCV, the redox reaction involves proton release and absorption, making pH a critical factor in its electrochemical detection.

Fig. 4 presents the DPVs of 750 nM VGCV at various pH ranging from 2 to 11. The results show that as the pH increases, the oxidation of VGCV occurs more readily, with the oxidation peaks shifting towards lower potentials. This behavior suggests that higher pH values facilitate the oxidation process. Between pH 2 and 8, the peak current increases, indicating enhanced oxidation. However, beyond pH 8, the peak current stabilizes,

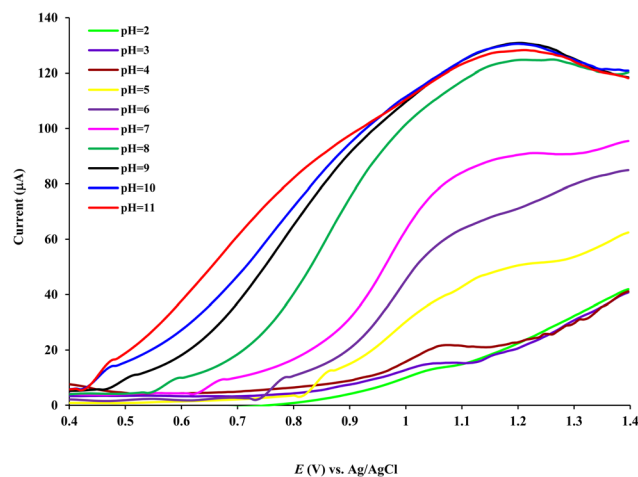


Fig. 4 DPVs obtained for 0.75  $\mu\text{M}$  VGCV in phosphate buffer solution at different pH values.

and only a shift in potential is observed. The shift towards more negative potentials, along with the increase in current, aligns with the expected behavior of VGCV's redox reaction.

The optimal pH for detecting VGCV was determined to be pH 7. Although pH 8 produced a higher peak, it was not selected due to the excessive broadening of the peak and the unsuitability of basic conditions for the drug's redox reaction. Fig. 5(a) illustrates the relationship between the oxidation peak current and pH for 750 nM VGCV, measured at a scan rate of 100 mV s<sup>-1</sup>. The oxidation peak current is weak in acidic conditions but increases with rising pH until it plateaus.

Fig. 5(b) highlights the linear range between pH 4 and 8, where a clear linear increase in peak current is observed at five specific pH values, further confirming the pH dependence of VGCV's electrochemical behavior. This analysis emphasizes the importance of pH optimization in achieving accurate and sensitive detection of VGCV using the Co-Ni(MLNW)/CPE sensor.

**3.2.3. Effect of scan rate on the electrochemical response of Co-Ni(MLNW)/CPE sensor.** The influence of scan rate on the electrochemical behavior of VGCV was investigated using the Co-Ni(MLNW)/CPE sensor. The study explored the redox response of 15 nM VGCV in phosphate buffer solution (pH 7.4) across a range of scan rates from 10 to 330 mV s<sup>-1</sup>, as depicted in Fig. 6(a). The results indicate that the electron transfer during the oxidation-reduction of VGCV is predominantly controlled by diffusion processes. The cyclic voltammetry (CV) method, which is particularly well-suited for examining the behavior of new pharmaceutical compounds, was utilized to assess the sensor's response under varying scan rates. This method provides valuable insights into the metabolic fate of the drug.

The oxidation peak current exhibited a linear increase ( $R^2 = 0.991$ ) with the square root of the potential scan rate, following the relationship  $I_p = 760.52v^{1/2} - 59.399$  (Fig. 6(b)). This indicates that the electrochemical oxidation of VGCV on the modified electrode surface is primarily governed by diffusion.<sup>29</sup>

The oxidative behavior of VGCV observed in this study is consistent with the previously reported oxidation mechanisms of guanine and guanosine, which suggests a comparable



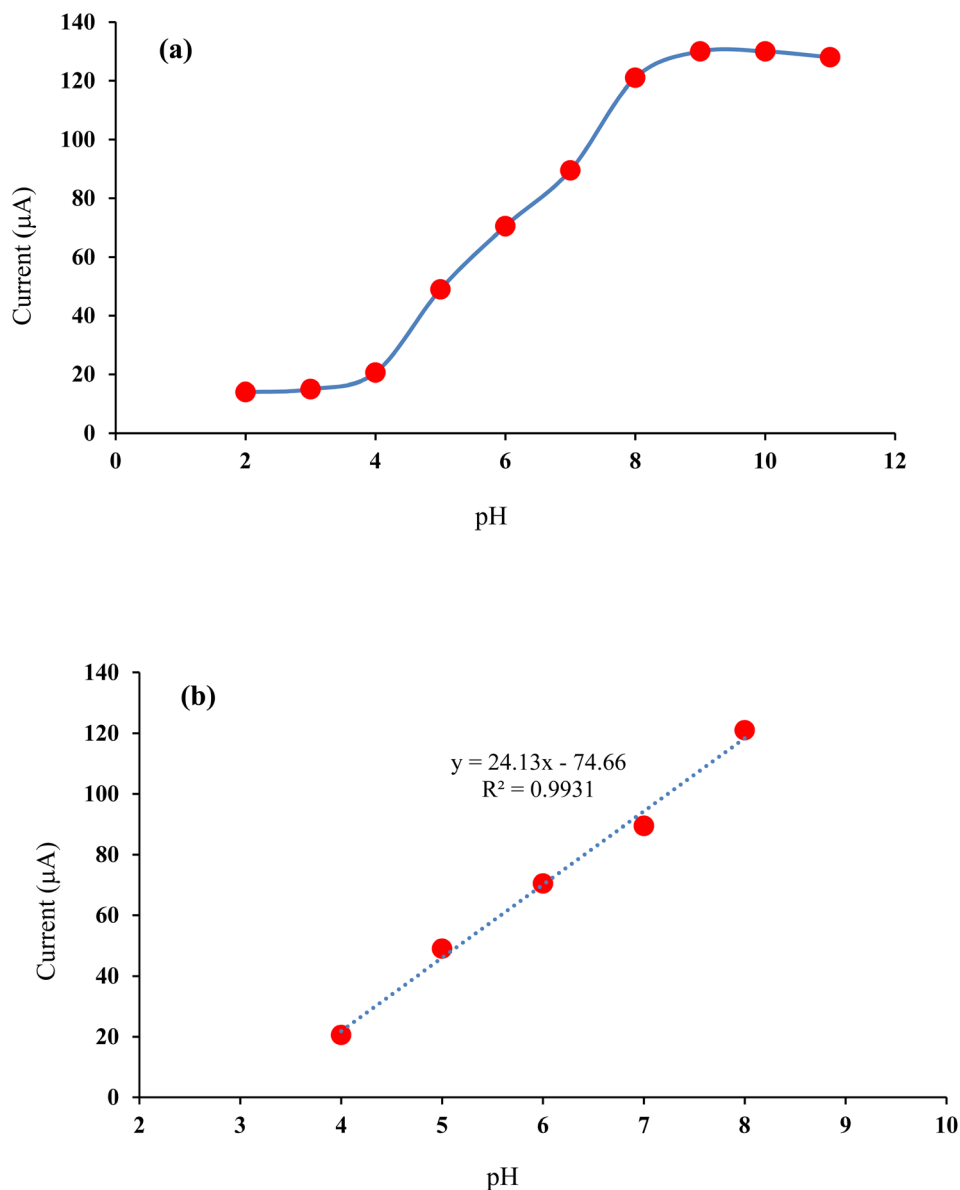


Fig. 5 (a) Influence of pH on the peak current ( $I_p$ ) for a solution with  $0.75 \mu\text{M}$  VGCV in phosphate buffer; (b) the linear range between pH 4 and 8.

electrochemical pathway. Scheme 2 illustrates the proposed oxidation mechanism of VGCV, which aligns well with the experimental results obtained in this research. The correlation between the scan rate and the electrochemical response further underscores the importance of optimizing scan rates to enhance the sensitivity and accuracy of VGCV detection using the Co-Ni(MLNW)/CPE sensor.

### 3.3. Electrochemical determination of VGCV

The voltammetric behavior of the modified electrode in response to varying concentrations of VGCV was analyzed using DPV measurements, with successive additions of different VGCV concentrations to phosphate buffer under optimal conditions (pH 7.4 and a scan rate of  $100 \text{ mV s}^{-1}$ ) (Fig. 7(a)). A standard calibration curve for VGCV was generated using DPV data. As shown in Fig. 7, the peak current increases as the VGCV

concentration rises. The developed electrode displayed a linear response over a wide concentration ranges of VGCV from  $0.1 \text{ nM}$  to  $2000 \text{ nM}$  (Fig. 7(b)).

The linear relationship between VGCV concentration and the peak current was established with the equation:

$$I_p (\mu\text{A}) = 0.1042[\text{VGCV (nM)}] + 12.738, R^2 = 0.9994 \quad (1)$$

where  $I_p$  represents the oxidation current and  $[\text{VGCV (nM)}]$  represents the concentration of VGCV. The calibration curve exhibited excellent linearity with a correlation coefficient of  $0.9972$ , indicating the sensor's high sensitivity and reliability. The limit of detection (LOD) and limit of quantification (LOQ) were determined to be  $0.03 \text{ nM}$  and  $0.1 \text{ nM}$  respectively. The performance of this electrode was compared with recent studies on VGCV detection (Table 1), demonstrating excellent performance at lower costs and with a simpler procedure.



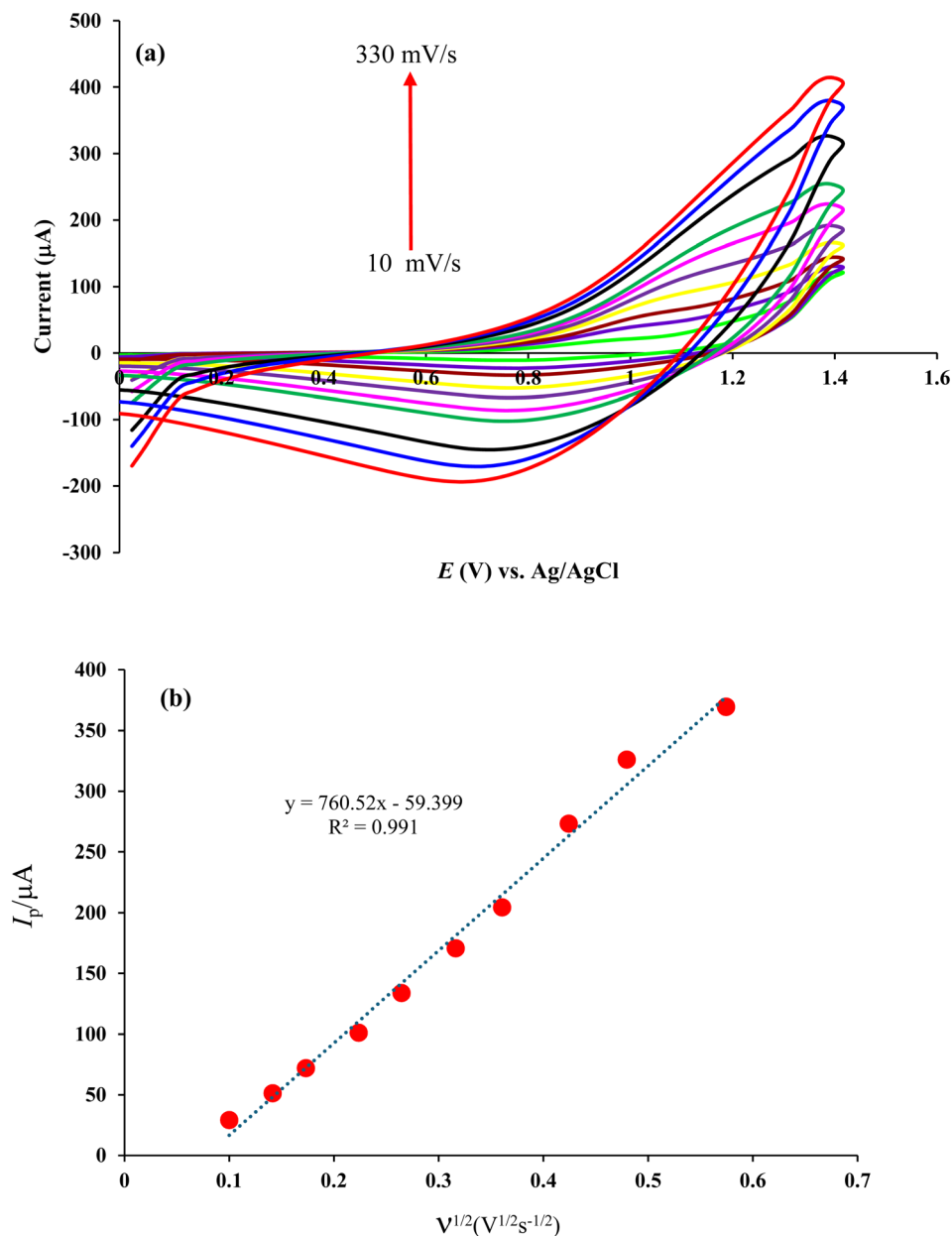


Fig. 6 (a) CVs of 10 nM VGCV in 0.1 M phosphate buffer solution (pH = 7.4) at different scan rates of 10, 20, 30, 50, 70, 100, 130, 180, 230 and 330  $\text{mV s}^{-1}$ ; (b) corresponding plot of oxidation peak current vs. square root of potential scan rate.

The sensor demonstrated a broad linear range from 0.1 nM to 2000 nM, with a remarkably low detection limit, making it highly effective for detecting VGCV even at trace levels. This performance is significant for accurately determining the drug dosage, highlighting the sensor's potential in clinical applications.

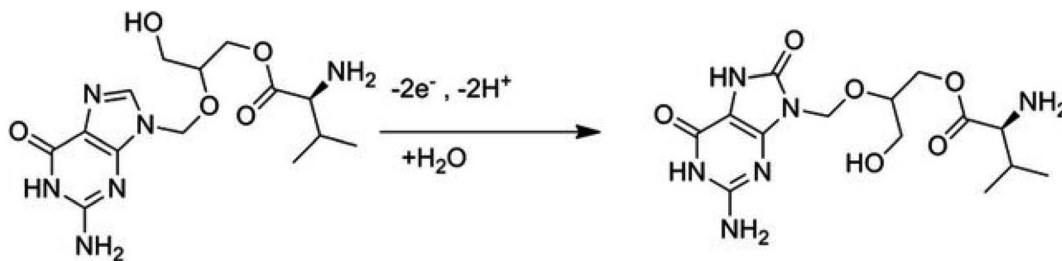
### 3.4. Stability and reproducibility

The Co-Ni(MLNW)/CPE sensor demonstrated excellent stability and reproducibility for the electrochemical measurement of VGCV. The sensor retained about 91% of its initial current response after 35 days of storage at room temperature, indicating its high stability, which is crucial for long-term applications (Fig. 8).

The sensor exhibited a rapid response time, reaching 95% of its maximum reduction current within just 5 seconds, making it suitable for quick measurements. Reproducibility was assessed by performing 30 consecutive measurements of a 600 nM VGCV solution, showing consistent current responses with a recovery rate ranging from 97.7% to 101.0%, which underscores the method's reliability and precision (Fig. 9).

Additionally, the relative standard deviation (RSD) for VGCV at a concentration of 30  $\mu\text{M}$  was found to be 4.5%, based on measurements using 10 freshly prepared electrodes. This low RSD reflects the high reproducibility of the electrode modification process employed in this study. The favorable electrocatalytic response of the Co-Ni(MLNW)/CPE electrode to VGCV





Scheme 2 VGCV oxidation mechanism at Co-Ni(MLNW)/CPE surface.

is attributed to the large electroactive surface area provided by the Ni-Co(MLNW) nanowires, enhancing the sensor's performance.

### 3.5. Interference study

To assess the practical applicability of the proposed Co-Ni(MLNW)/CPE sensor for the determination of VGCV in real

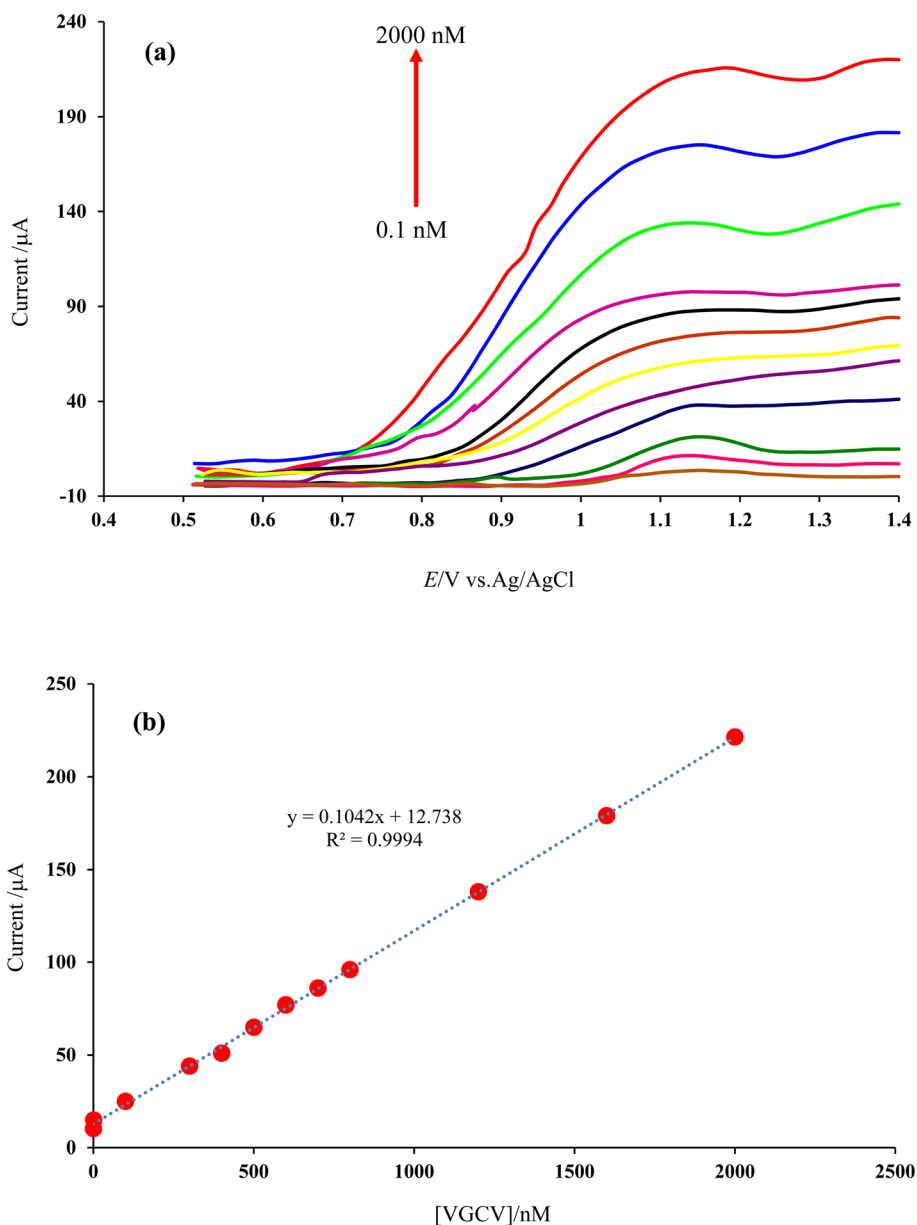


Fig. 7 (a) DPVs of different concentrations of VGCV from 0.1 to 2000 nM in 0.1 M phosphate buffer solution (pH = 7.4); (b) resulted standard calibration curve. Error bars obtained for three trials.



Table 1 A comparison of LOD and LDR values for determination of VGCV by Ni–Co(MLNW)/CPE with other reported methods

Method	Electrode	LDR	LOD	Ref.
DPV	AuNP-MIP/MWCNT/GCE	1–500 nM 500–2000 nM	0.3 nM	30
DPV	ERGO-GCE	15 nM–35 $\mu$ M	3.1 nM	31
AdSDPV	MWCNT-GCE	7.5 nM–1.0 $\mu$ M	1.52 nM	32
DPV	NF/Fe <sub>3</sub> O <sub>4</sub> -Gr/GCE	0.005–1.8 $\mu$ M 1.8–6 $\mu$ M	2.9 nM	33
SWV	BNC/CPE	60 nM–300 $\mu$ M	13.5 nM	34
SWV	g-C <sub>3</sub> N <sub>4</sub> /CPE	1–16 $\mu$ M	8.8 nM	35
SWV	GRP-Bi <sub>2</sub> O <sub>3</sub> /GCE	100–700 ng mL <sup>-1</sup>	15.53 ng mL <sup>-1</sup>	36
DPV	Ni–Co(MLNW)/CPE	0.1–2000 nM	0.03 nM	This work

samples, an interference study was conducted. This study aimed to evaluate the sensor's selectivity by examining the effect of various potentially interfering species commonly present in biological fluids. The interference was tested by introducing the sensor into solutions containing a fixed concentration of VGCV (10  $\mu$ M) along with varying concentrations of potential interfering substances. A relative error of less than 3% in the VGCV signal was considered acceptable for determining the interference threshold.

The results indicated that common metal ions such as Fe<sup>2+</sup>, Ca<sup>2+</sup>, Mg<sup>2+</sup>, and Cu<sup>2+</sup>, up to 200 times their concentration, did not significantly affect the VGCV signal. Additionally, ascorbic acid and uric acid, at 50 times their concentration, showed no interference with the oxidation signal of VGCV on the modified electrode.

These findings suggest that the Ni–CoMULNW-modified electrode exhibits high selectivity and is largely unaffected by many common interfering species, making it suitable for accurate VGCV measurement in real biological samples.

### 3.6. Determination of VGCV in real samples

To demonstrate the practical applicability of the proposed Co–Ni(MLNW)/CPE sensor for analyzing real samples, it was employed to determine VGCV in human plasma samples. The

plasma samples were first prepared and then diluted with 0.05 M phosphate buffer solution at pH 7. The analysis was performed using the standard addition method.

Initially, the concentration of VGCV in the prepared plasma samples was determined. Subsequently, known amounts of VGCV were added to the samples, and the concentration was measured again. The results, presented in Table 2, showed an average recovery rate of 97% for the added VGCV, indicating the high accuracy of the proposed sensor.

The high recovery percentage underscores the reliability of the Co–Ni(MLNW)/CPE sensor for VGCV detection, making it a promising tool for measuring VGCV in biological samples. The recovery rate was calculated using the following formula:

$$\text{Recovery(\%)} = \left( \frac{\text{measured value} - \text{expected value}}{\text{expected value}} \times 100 \right) + 100 \quad (2)$$

This high accuracy makes the proposed sensor a valuable option for researchers conducting VGCV measurements in biological samples.

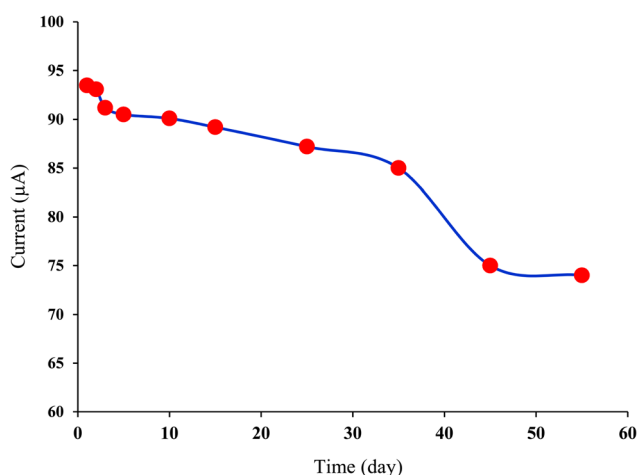


Fig. 8 Sensor response ( $I_p$ ) to a solution of valganciclovir with 600 nM concentration over a period of 55 days after fabrication and storage at room temperature at pH = 7 and a scan rate of 100 mV s<sup>-1</sup>.

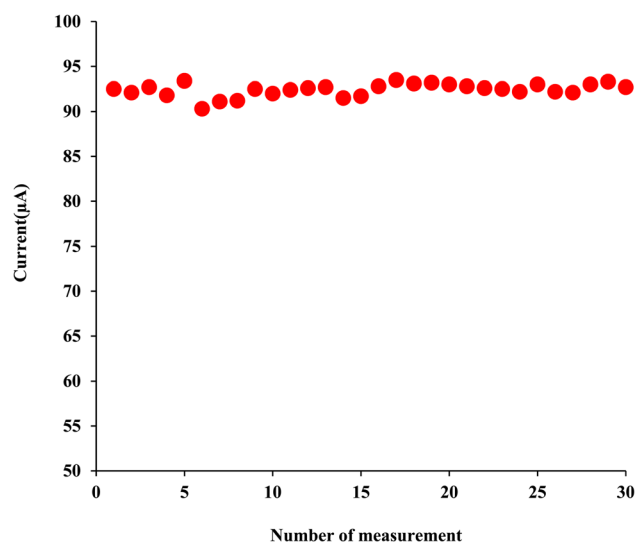


Fig. 9 Response of the designed sensor to a solution of valganciclovir with 600 nM concentration in 30 consecutive measurements at pH = 7 and a scan rate of 100 mV s<sup>-1</sup>.



**Table 2** Results of recovery tests for determination of VGCV spiked in buffer solution by DPV technique using Ni–Co(MLNW)/CPE

Sample	Added ( $\mu\text{M}$ )	Found ( $\mu\text{M}$ )	Recovery (%)
S <sub>0</sub>	0	0.01	—
S <sub>1</sub>	2	1.91 $\pm$ 0.07	95.0
S <sub>2</sub>	5	4.91 $\pm$ 0.10	98.0
S <sub>3</sub>	10	9.81 $\pm$ 0.11	98.0

## 4. Conclusion

In summary, a novel sensor based on a carbon paste electrode modified with Ni–Co nanowires was developed for the detection of VGCV. The Ni–Co nanowires were synthesized using a controlled electrodeposition method with an AAO template. Both layered and alloyed Ni–Co nanowires were prepared and compared as electrode modifiers through differential pulse voltammetry (DPV). The Ni–CoMULNW demonstrated superior performance over Ni–CoALINW. The structure of Ni–CoMULNW was characterized using scanning electron microscopy (SEM) and energy-dispersive X-ray spectroscopy (EDX). Following the complete dissolution of the template, the resulting nanowires were used to modify the carbon paste electrode. The modified electrodes were then evaluated using cyclic voltammetry (CV) and DPV. The proposed sensor exhibited accurate and rapid response to VGCV, with notable features including a wide linear range of 0.1 to 2000 nM, a low detection limit of 0.03 nM, high reproducibility (4.5%), and a high average recovery of 97.9% in human plasma samples. Additionally, it showed minimal interference from common potential interfering species. These results highlight the clear, stable, and effective electrocatalytic response of the Ni–CoMULNW modified carbon paste electrode, making it a suitable and reliable tool for VGCV measurement. Compared to previously reported methods, the Ni–Co MLNW/CPE offers a combination of high sensitivity, good stability, and ease of fabrication, making it a potentially valuable tool for VGCV monitoring in clinical settings. Furthermore, the use of a carbon paste electrode platform offers advantages in terms of cost-effectiveness and disposability.

## Data availability

The data that support the findings of this study are available on request from the corresponding author.

## Author contributions

Maedeh Malekzadeh: investigation, methodology, visualization, writing – original draft, data curation, formal analysis, software. Amir Abbas Rafati: project administration, conceptualization, supervision, funding acquisition, writing – review & editing, resource, validation. Ahmad Bagheri: Advisor, data interpretation, reviewed and edited the manuscript. All authors read and approved the final manuscript.

## Conflicts of interest

The authors declare that they have no known competing financial interests or personal relationships that could have appeared to influence the work reported in this paper.

## Acknowledgements

The authors greatly acknowledge Bu-Ali Sina University for the financial support from the Grant Research Council.

## References

- D. Mondal, Valganciclovir, *Reference Module in Biomedical Sciences*, 2016, DOI: [10.1016/B978-0-12-801238-3.99406-6](https://doi.org/10.1016/B978-0-12-801238-3.99406-6).
- A. Galar, M. Valerio, P. Catalán, X. García-González, A. Burillo, A. Fernández-Cruz, E. Zataráin, I. Sousa-Casasnovas, F. Anaya, M. L. Rodríguez-Ferrero, P. Muñoz and E. Bouza, Valganciclovir–Ganciclovir use and systematic therapeutic drug monitoring. An invitation to antiviral stewardship, *Antibiotics*, 2021, **10**(1), 77, DOI: [10.3390/antibiotics10010077](https://doi.org/10.3390/antibiotics10010077).
- V. Ganesh, K. Sahini, P. Poorna Basuri and C. N. Nalini, Review of analytical and bioanalytical techniques for the determination of first-line anticytomegalovirus drugs, *Chin. J. Anal. Chem.*, 2022, **50**(8), 100123, DOI: [10.1016/j.cjac.2022.100123](https://doi.org/10.1016/j.cjac.2022.100123).
- S. Sawant and V. Barge, A validated stability indicating RP-HPLC method for valganciclovir, identification and characterization of forced degradation products of valganciclovir using LC-MS/MS, *Acta Chromatogr.*, 2014, **26**(1), 29–42, DOI: [10.1556/achrom.26.2014.1.4](https://doi.org/10.1556/achrom.26.2014.1.4).
- G. V. Abhigna and R. Sundararajan, Analytical method development and validation for determination of valganciclovir by using RP-HPLC, *Int. J. Pharm. Invest.*, 2023, **13**(3), 617–624, DOI: [10.5530/ijpi.13.3.076](https://doi.org/10.5530/ijpi.13.3.076).
- S. Sanlı, N. Sanlı and C. Lunte, Determination and validation of capillary electrophoretic and liquid chromatographic methods for concurrent assay of valganciclovir and lamivudine in pharmaceutical formulations, *Curr. Pharm. Anal.*, 2017, **13**(1), 31–38, DOI: [10.2174/1573412912666160728153846](https://doi.org/10.2174/1573412912666160728153846).
- S. Abedini, A. A. Rafati and A. Ghaffarinejad, A simple and low-cost electrochemical sensor based on a graphite sheet electrode modified by carboxylated multiwalled carbon nanotubes and gold nanoparticles for detection of acyclovir, *New J. Chem.*, 2022, **46**, 20403–20411, DOI: [10.1039/D2NJ04065D](https://doi.org/10.1039/D2NJ04065D).
- G. Muungani and W. E. van Zyl, A CaCuSi<sub>4</sub>O<sub>10</sub>/GCE electrochemical sensor for detection of norfloxacin in pharmaceutical formulations, *RSC Adv.*, 2023, **13**, 12799–12808, DOI: [10.1039/D3RA01702H](https://doi.org/10.1039/D3RA01702H).
- A. A. Mouhamed, B. M. Eltanany, N. M. Mostafa, T. A. Elwaie and A. H. Nadim, Design of screen-printed potentiometric platform for sensitive determination of mirabegron in spiked human plasma; molecular docking and transducer



- optimization, *RSC Adv.*, 2023, **13**, 23138–23146, DOI: [10.1039/D3RA02343E](https://doi.org/10.1039/D3RA02343E).
- 10 H. A. M. Nouredin, A. M. Abdel-Aziz, M. M. Mabrouk, A. H. K. Saad and I. H. A. Badr, Green and cost-effective voltammetric assay for spiramycin based on activated glassy carbon electrode and its applications to urine and milk samples, *RSC Adv.*, 2023, **13**, 844–852, DOI: [10.1039/D2RA06768D](https://doi.org/10.1039/D2RA06768D).
- 11 B. M. Tuchia, R. I. Stefan-van Staden and J. K. Frederick van Staden, Stochastic platform based on calix[6]arene and TiO<sub>2</sub>-modified reduced graphene oxide electrode for on-site determination of nonivamide in pharmaceutical and water samples, *RSC Adv.*, 2023, **13**, 17628–17632, DOI: [10.1039/D3RA02363J](https://doi.org/10.1039/D3RA02363J).
- 12 R. A. Joghani, A. A. Rafati, J. Ghodsi, P. Assari and A. Feizollahi, A sensitive voltammetric sensor based on carbon nanotube/nickel nanoparticle for determination of daclatasvir (an anti-hepatitis C drug) in real samples, *J. Appl. Electrochem.*, 2020, **50**, 1199–1208, DOI: [10.1007/s10800-020-01478-1](https://doi.org/10.1007/s10800-020-01478-1).
- 13 J. Kouhdareh, R. Karimi-Nami, H. Keypour, K. Rabiei, S. Alavinia, S. Ghahri Saremid and M. Noroozi, Synthesis of a Au/Au NPs-PPy/l-CYs/ZIF-8 nanocomposite electrode for voltammetric determination of insulin in human blood, *RSC Adv.*, 2023, **13**, 24474–24486, DOI: [10.1039/D3RA04064J](https://doi.org/10.1039/D3RA04064J).
- 14 A. K. Tawade, A. P. Khairnar, J. V. Kamble, A. R. Kadam, K. K. K. Sharma, A. A. Powar, V. S. Patil, M. R. Patil, S. S. Mali, C. Kook Hong and S. N. Tayade, Designing a TiO<sub>2</sub>-MoO<sub>3</sub>-BMIMBr nanocomposite by a solvohydrothermal method using an ionic liquid aqueous mixture: an ultra high sensitive acetaminophen sensor, *RSC Adv.*, 2023, **13**, 21283–21295, DOI: [10.1039/D3RA02611F](https://doi.org/10.1039/D3RA02611F).
- 15 M. Nosrati, A. A. Rafati, A. Bagheri and P. Assari, First report for the voltammetric determination of Lamivudine anti-HIV drug in tablet dosage forms by glassy carbon electrode modified with polyaniline nanowires, *Appl. Phys. A*, 2024, **130**, 701, DOI: [10.1007/s00339-024-07827-7](https://doi.org/10.1007/s00339-024-07827-7).
- 16 B. Habibi, S. Pashazadeh, A. Pashazadeh and L. A. Saghatforoush, An amplified electrochemical sensor employing one-step synthesized nickel-copper-zinc ferrite/carboxymethyl cellulose/graphene oxide nanosheets composite for sensitive analysis of omeprazole, *RSC Adv.*, 2023, **13**, 29931–29943, DOI: [10.1039/D3RA04766K](https://doi.org/10.1039/D3RA04766K).
- 17 F. Yang, Y. Ai, X. Li, L. Wang, Z. Zhang, W. Ding and W. Sun, Preparation of electrochemical horseradish peroxidase biosensor with black phosphorene-zinc oxide nanocomposite and their applications, *RSC Adv.*, 2023, **13**, 32028–32038, DOI: [10.1039/D3RA05148J](https://doi.org/10.1039/D3RA05148J).
- 18 A. Feizollahi, A. A. Rafati, P. Assari and R. Asadpour Joghani, Simple and fast determination of piroxicam in pharmaceutical and real samples using glassy carbon electrode modified with copper nano-particles, *J. Electrochem. Soc.*, 2020, **167**, 067521, DOI: [10.1149/1945-7111/ab82f9](https://doi.org/10.1149/1945-7111/ab82f9).
- 19 A. Feizollahi, A. A. Rafati, P. Assaria and R. Asadpour Joghani, Development of an electrochemical sensor for the determination of antibiotic sulfamethazine in cow milk using graphene oxide decorated with Cu-Ag core-shell nanoparticles, *Anal. Methods*, 2021, **13**, 910–917, DOI: [10.1039/D0AY02261F](https://doi.org/10.1039/D0AY02261F).
- 20 M. HosseinAbadi, A. A. Rafati and E. Ghasemian Lemraski, Electrochemical detection of regorafenib using a graphite sheet electrode modified with nitrogen-doped reduced graphene oxide nanocomposite, *Mater. Sci. Eng. B*, 2024, **304**, 117375, DOI: [10.1016/j.mseb.2024.117375](https://doi.org/10.1016/j.mseb.2024.117375).
- 21 Y. J. Chang, J. M. Dou and S. H. Yeh, Effects of nickel-cobalt material properties on glucose catalysis, *Microchem. J.*, 2022, **182**, 107950, DOI: [10.1016/j.microc.2022.107950](https://doi.org/10.1016/j.microc.2022.107950).
- 22 M. Hussain, A. Nisar, L. Qian, S. Karim, M. Khan, Y. Liu, H. Sun and M. Ahmad, Ni and Co synergy in bimetallic nanowires for the electrochemical detection of hydrogen peroxide, *Nanotechnol.*, 2021, **32**, 205501, DOI: [10.1088/1361-6528/abe4fb](https://doi.org/10.1088/1361-6528/abe4fb).
- 23 Y. Liu, J. Guan, W. Chen, Y. Wu, S. Li, X. Du and M. Zhang, Nickel-cobalt derived nanowires/nanosheets as electrocatalyst for efficient H<sub>2</sub> generation via urea oxidation reaction, *J. Alloys Compd.*, 2022, **891**, 161790, DOI: [10.1016/j.jallcom.2021.161790](https://doi.org/10.1016/j.jallcom.2021.161790).
- 24 S. J. Malode, P. Sharma, M. R. Hasan, N. P. Shetti and R. J. Mascarenhas, 4-Carbon and carbon paste electrodes, in *Woodhead Publishing Series In Electronic And Optical Materials, Electrochemical Sensors*, ed. G. Maruccio and J. Narang, Woodhead Publishing, 2022, pp. 79–114, DOI: [10.1016/B978-0-12-823148-7.00004-0](https://doi.org/10.1016/B978-0-12-823148-7.00004-0).
- 25 R. Rejithamol and S. Beena, Carbon paste electrochemical sensors for the detection of neurotransmitters, *Front. Sens.*, 2022, **3**, 901628, DOI: [10.3389/fsens.2022.901628](https://doi.org/10.3389/fsens.2022.901628).
- 26 M. García, P. Batalla and A. Escarpa, Metallic and polymeric nanowires for electrochemical sensing and biosensing, *TrAC, Trends Anal. Chem.*, 2014, **57**, 6–22, DOI: [10.1016/j.trac.2014.01.004](https://doi.org/10.1016/j.trac.2014.01.004).
- 27 B. Kashyap and R. Kumar, A novel multi-set differential pulse voltammetry technique for improving precision in electrochemical sensing, *Biosens. Bioelectron.*, 2022, **216**, 114628, DOI: [10.1016/j.bios.2022.114628](https://doi.org/10.1016/j.bios.2022.114628).
- 28 P. G. Schiavi, P. Altimari, A. Rubino and F. Pagnanelli, Electrodeposition of cobalt nanowires into alumina templates generated by one-step anodization, *Electrochim. Acta*, 2018, **259**, 711–722, DOI: [10.1016/j.electacta.2017.11.035](https://doi.org/10.1016/j.electacta.2017.11.035).
- 29 M. Mazloum-Ardakani, Z. Taleat, A. Khoshroo, H. Beitollahi and H. Dehghani, Electrocatalytic oxidation and voltammetric determination of levodopa in the presence of carbidopa at the surface of a nanostructure based electrochemical sensor, *Biosens. Bioelectron.*, 2012, **35**(1), 75–81, DOI: [10.1016/j.bios.2012.02.014](https://doi.org/10.1016/j.bios.2012.02.014).
- 30 M. B. Gholivand and M. Torkashvand, The fabrication of a new electrochemical sensor based on electropolymerization of nanocomposite gold nanoparticle-molecularly imprinted polymer for determination of



- valganciclovir, *Mater. Sci. Eng. C*, 2016, **59**, 594–603, DOI: [10.1016/j.msec.2015.09.016](https://doi.org/10.1016/j.msec.2015.09.016).
- 31 S. N. Prashanth, N. L. Teradal, J. Seetharamappa and A. K. Satpati, Fabrication of an electrochemical sensor based on electroreduced graphene oxide for the determination of valganciclovir, *J. Electrochem. Soc.*, 2014, **161**(6), B117, DOI: [10.1149/2.010406jes](https://doi.org/10.1149/2.010406jes).
- 32 B. Dogan-Topal, B. Bozal-Palabiyik, B. Uslu and S. A. Ozkan, Multi-walled carbon nanotube modified glassy carbon electrode as a voltammetric nanosensor for the sensitive determination of anti-viral drug valganciclovir in pharmaceuticals, *Sens. Actuators, B*, 2013, **177**, 841–847, DOI: [10.1016/j.snb.2012.11.111](https://doi.org/10.1016/j.snb.2012.11.111).
- 33 E. Ahmadi and M. B. Gholivand, Sensitive determination of the anti-viral drug valganciclovir by a nafion/magnetic nanoparticlegraphene/GCE as a voltammetric sensor, *Anal. Methods*, 2019, **11**, 4659–4667, DOI: [10.1039/C9AY01046G](https://doi.org/10.1039/C9AY01046G).
- 34 Y. M. Shanbhag, S. Dhanalakshmi, M. M. Shanbhag, A. N. Alodhayb and N. P. Shetti, Bentonite clay/carbon matrix-based voltammetric sensor for the detection of valganciclovir, *Inorg. Chem. Commun.*, 2024, **169**, 113079, DOI: [10.1016/j.inoche.2024.113079](https://doi.org/10.1016/j.inoche.2024.113079).
- 35 M. Sreenivasulu, S. J. Malode, A. N. Alodhayb and N. P. Shetti, Exfoliated 2-D graphitic carbon nitride nanosheets for electrochemical detection of the antiviral drug valganciclovir, *Electrocatalysis*, 2024, **15**, 456–473, DOI: [10.1007/s12678-024-00887-6](https://doi.org/10.1007/s12678-024-00887-6).
- 36 R. Jain and P. Pandey, Electrocatalytic quantification of antiviral drug valacyclovir, *Ionics*, 2015, **21**, 3279–3287, DOI: [10.1007/s11581-015-1511-2](https://doi.org/10.1007/s11581-015-1511-2).

